ISI Web of Knowledge℠

Journal Citation Reports®

WELCOME HELP

2012 JCR Science Edition

Journal Summary List

Journal Title Changes

Journals from: search ISSN for '1420-2026'

Sorted by: Journal Title SORT AGAIN

Journals 1 - 1 (of 1) [1] **Page 1 of 1**

MARK ALL UPDATE MARKED LIST ***Ranking is based on your journal and sort selections.***

Mark	Rank	Abbreviated Journal Title *(linked to journal information)*	ISSN	JCR Data						*Eigenfactor®* Metrics	
				Total Cites	Impact Factor	5-Year Impact Factor	Immediacy Index	Articles	Cited Half-life	*Eigenfactor®* Score	*Article Influence®* Score
☐	1	ENVIRON MODEL ASSESS	1420-2026	525	0.977	1.114	0.098	51	6.3	0.00131	0.342

MARK ALL UPDATE MARKED LIST

Journals 1 - 1 (of 1) [1] **Page 1 of 1**

Acceptable Use Policy
Copyright © 2014 Thomson Reuters.

THOMSON REUTERS

Published by Thomson Reuters

Environ Model Assess (2014) 19:139–152
DOI 10.1007/s10666-013-9381-3

Analysis of Key Features of Non-Linear Behaviour Using Recurrence Quantification. Case Study: Urban Airborne Pollution at Mexico City

Marco A. Aceves-Fernandez · J. Carlos Pedraza-Ortega · Artemio Sotomayor-Olmedo · Juan M. Ramos-Arreguín · J. Emilio Vargas-Soto · Saul Tovar-Arriaga

Received: 3 March 2012 / Accepted: 21 August 2013 / Published online: 10 September 2013
© Springer Science+Business Media Dordrecht 2013

Abstract The use of recurrence plots have been extensively used in various fields. In this work, recurrence plots investigate the changes in the non-linear behaviour of urban air pollution using large datasets of raw data (hourly). This analysis has not been used before to extract information from large datasets for this type of non-linear problem. Two different approaches have been used to tackle this problem. The first approach is to show results according to monitoring network. The second approach is to show the results by particle type. This analysis shows the feasibility of using recurrence analysis for pollution monitoring and control.

Keywords Recurrence plot · Air quality · Air pollution modelling · Atmospheric pollution · Recurrence quantification analysis

1 Introduction

The states in nature typically change in time. The importance in the investigation of these changes in complex systems helps to understand and describe such changes. A relatively new method based on non-linear data analysis has become popular to describe the changes of these systems. This method is called recurrence plot [13, 44].

In this contribution, the non-linear behaviour of urban air pollution is quantified and analysed at various sites at Mexico City, using large datasets over a number of years. This is carried out to show the feasibility of analysing key features embedded in the raw datasets.

M. A. Aceves-Fernandez (✉) · J. C. Pedraza-Ortega · A. Sotomayor-Olmedo · J. M. Ramos-Arreguín · J. E. Vargas-Soto · S. Tovar-Arriaga
Universidad Autonoma de Queretaro, Campus Juriquilla, Av. de las Ciencias S/N, Juriquilla, Delegación Santa Rosa Jauregui, Santiago de Querétaro 76230, Querétaro, Mexico
e-mail: marco.aceves@gmail.com

2 Background

2.1 Urban Airborne Pollution

In recent times, urban air pollution has been a growing problem especially for urban communities. Size, shape, and chemical properties are one of the main factors governing the lifetime of particles in the atmosphere and the site of deposition within the respiratory tract. Also, air pollution has been held responsible for various health disorders, especially respiratory complications, resulting in an increase in the number of asthmatic cases and hospital admissions in some parts of the world and has been widely documented [6, 18, 23, 49].

Most major pollutants can alter pulmonary function in addition to other health effects when the exposure concentrations are high. This is especially severe in vulnerable sectors of the population such as asthmatic children and the elderly and has been vastly documented [21, 22, 34, 42].

The atmosphere of Mexico City has received considerable scientific attention in recent years, mainly because of concerns about the potential health effects of air pollutants on its more than 20 million inhabitants [40]

In this work, five different gases were chosen due to the site's availability and toxicity: ozone (O_3), carbon monoxide (CO), nitrogen dioxide (NO_2), sulphur dioxide (SO_2), and particulate matter of less than 10 μm (PM_{10}). The datasets are separated according to the month of the year and type of particle. There is one data for each hour and for each particle for all sites at Mexico City, making it difficult to extract information from datasets using common methods.

O_3 is a natural atmosphere component that is found on low concentrations and is crucial for life. Air pollution caused by high concentrations of ozone is a common problem in large cities throughout the world [9]. Mexico City is among the ones suffering from this problem.

In Mexico City, there is a decrease of ozone levels especially from 2009. However, there is still a risky situation for overexposure mainly in the southwest region [38], according to the official Mexican air quality standards [29],

It is a well-known fact that individuals exposed for a long period of time to high concentrations of ozone may experience serious health problems [4, 46]. Epidemiology studies have found associations between daily ozone levels and hospital admissions [7, 33]. This pollutant is associated with respiratory symptoms, specially coughing. This is aggravated in patients with asthma [30].

CO is a tasteless, odourless, gaseous pollutant ubiquitous in the outdoor atmosphere that is generated by combustion [47]. CO is produced by incomplete combustion of hydrocarbons. Its main source is vehicle exhaust emissions; secondary important sources are industry, heating, and fires. The concentrations of CO as well as their fluctuations are related to a large extent to the circulation of cars [37].

In Mexico, the official norm: NOM-021-SSA1-1993 sets the maximum level for carbon monoxide on 11.0 ppm for an average of 8 h, which cannot be exceeded more than once a year. Comparatively, in the USA, the federal standard is 9 ppm for 8 h and 35 ppm for a 1-h average.

Adverse health effects of CO exposure include death from asphyxiation at high-exposure levels and at lower levels, impaired neuropsychological performance, and risk for myocardial ischemia and rhythm disturbances in persons with cardiovascular disease. The most definitive evidence on CO comes largely from controlled exposure studies, involving CO inhalation at concentrations to mimic exposures previously typical of urban environments [8, 11]

Also, carbon monoxide has been held responsible for many hospital admissions due to carbon monoxide poisoning. Only in the USA, around 40,000 people are admitted in hospitals for this cause in 1 year [45].

NO_2 is a particularly important compound, not only for its health effects, but also because it absorbs visible light and contributes to visibility decrease. It also plays a critical role in the production of ozone since the photolysis of NO_2 is the initial step in the photochemical reaction of the ozone [9].

In Mexico, the official norm: NOM-023-SSA1-1993 establishes a maximum allowed concentration of 0.21 ppm hourly mean, which cannot be exceeded more than once a year. Comparatively, in the USA, the federal standard establishes a value of 0.053 ppm annual mean. The World Health Organization (WHO) recommends a value of 40 $\mu g/m^3$ (0.021 ppm) for annual mean and 200 $\mu g/m^3$ (0.106 ppm) for hourly mean.

By nature, there is a nitrogen dioxide concentration of 10 to 50 ppb. However, the high levels of nitrogen dioxide are due to industrial processes and fossil sources. Furthermore, motor vehicles substantially contribute to urban levels of nitrogen oxides through their engine combustion processes [15]. According to several authors, the monitoring of NO_2 is critically important in order to assess the potential effects of NO_2 on human health and ecosystems, as well as developing strategies for the effective control of NO_2 pollution (e.g. [3, 12, 43]).

SO_2 is ubiquitous in the biosphere and often occurs in relatively high concentrations in fossil fuels, with coal and crude oil deposits commonly containing 1–2 % sulphur by weight. The widespread combustion of fossil fuels has, therefore, greatly increased sulphur emissions into the atmosphere [39].

The World Health Organization recommends a concentration of between 100 and 150 $\mu g/m^3$ 24 h mean and 40 to 60 $\mu g/m^3$ annual mean. The Mexican official norm: NOM-022-SSA1-1993 establishes a limit of 341 $\mu g/m^3$ 24-h mean once a year and 79 $\mu g/m^3$ annual mean to protect the vulnerable population.

In the past three decades in Europe, and more recently in the USA, there have been substantial reductions in SO_2 emissions ([19, 48], among others).

Sulphur dioxide gases contribute to the deterioration of air quality. Several epidemiological studies have demonstrated a direct association between atmospheric inhalable sulphur dioxide and respiratory diseases, pulmonary damage, and mortality among population [35]. In urban environments, sulphur dioxide is generated by many sources. One of them is the burning of solid compounds or petroleum-derived products.

The airborne particulate matter (PM) is a mixture of small particles and liquid droplets suspended in the atmosphere, which contributes significantly to the urban air quality such as acid rain and visibility degradation [32]. A number of studies have linked health effects to air pollutants in residents of Mexico City. Air pollution has been associated with respiratory function and symptoms of susceptible populations, such as children, for example [17], and explicitly with fine PM ($PM_{2.5}$ and PM_{10}).

Asthmatic children are very susceptible to air pollution, and associations have been reported for the case of Mexico City. An increase of 20 $\mu g/m^3$ of PM_{10} was associated with an 8 % increase in lower respiratory illness in asthmatic children [36].

An airborne pollution particle could be any solid or liquid material with a diameter between 0.002 and 500 μm. Airborne particulates of 10-μm diameter and less are of concern from the perspective of air pollution. A variety of national and worldwide standards, directives, and guidelines exist to define acceptable particulate levels in the air.

These types of particles are classified according to their effect on human health and their physical characteristics.

2.2 Mexico's Sites

Mexico City is geographically located in the Valley of Mexico. This valley is a large valley in the high plateaus at the centre of Mexico. It has an altitude of 2,240 m (7,349 ft). The Federal District of Mexico City is situated in central-south Mexico and it is surrounded by the state of Mexico on the west, north, and east, and by the state of Morelos on the south. The city covers an area of around 1,485 km^2 (571 miles^2) with the elevation of 2,240 m (7,349 ft).

The sites used in this work are as follow: Northeast (San Agustín—SAG), Northwest (Acatlán—FAC), Downtown (Merced—MER), Southeast (Iztapalapa—UIZ) and Southwest (Pedregal—PED). The map of the monitoring sites is shown on Fig. 1.

3 Recurrence Plots

The recurrence plot (RP) exhibits characteristic patterns for typical dynamic behaviour. A collection of single recurrence points, homogeneously and irregularly distributed over the whole plot, reveals a mainly stochastic process [26].

Recurrence plot is a graphical tool introduced by Eckmann et al. [13] in order to extract qualitative characteristics of a time series. The recurrence of a state i at a different time j is pictured within a two-dimensional squared matrix with black and white dots, where the black dots represent a recurrence and both axes represent time [1, 53].

Such RP can be mathematically expressed as:

$$R_{i,j}^{m,\varepsilon^i} = \Theta\left(\varepsilon_i - \left\| \vec{X}_I - \vec{X}_J \right\|, \ \vec{X}_I \in \Re^m\right), \qquad i,j = 1..N, \ (1)$$

where N is the number of considered states x_i; ε_1 is a threshold distance, $\|\cdot\|$ a norm and Θ (.) the Heaviside function [14].

Since $R_{i,i}=1 (i=1\ldots N)$ by definition, the RP has a black main diagonal line called line of identity (LOI). In this context, the Heaviside function Θ (.) is a recurrence of a state $\overrightarrow{X_1}$ that is sufficiently close to $\overrightarrow{X_1}$ (states $\overrightarrow{X_1}$ that fall into an m-dimensional neighbourhood). In other words, the Heaviside function is a discontinuous function whose value is zero for negative argument and one for positive argument [10].

Using the time series of a single observable variable (gases, in this case), it is possible to reconstruct a phase space trajectory. Starting from the scalar time series $\{X_t\}_{t=1}^{T}$ a sequence of embedded vectors is $y(i) \equiv (x_i, x_{i+\tau}, x_{i+2\tau}, \ldots, x_{i+(m-1)\tau}$ generated [31]. The set of all embedded vectors $y(i), i = 1,\ldots,T-(m-1)\tau$, constitutes a trajectory in $\Re^m$ where m is the embedding dimension and τ is the time delay. Each

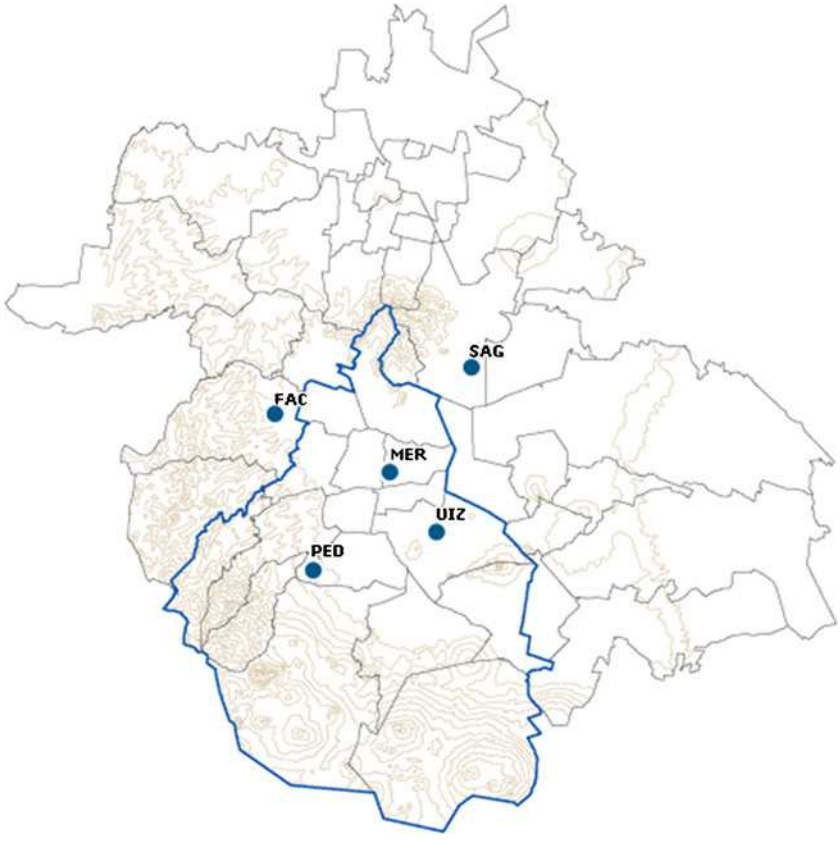

Fig. 1 Map for the monitoring sites at Mexico City

unknown point of the phase space at time I is reconstructed by the delayed vector $y(i)$ in an m-dimensional space called the reconstructed phase space.

Determining the embedding parameters must be the first step for analysing non-linear systems [2, 5, 16, 26, 31]. For this reason, a search for the best dimension and time delay must be made first. In this contribution, the best dimension value is calculated for each recurrence plot using the algorithm of false nearest neighbours as shown on [31, 54].

Also, when calculating an RP, a norm must be chosen [20]. The most widely used norms are the L1, L2 (Euclidean norm), and L∞ [51]. In this work, the Euclidean norm was used. Figure 2 shows the recurrence plots of a random signal, a sine wave and two RPs chosen randomly for airborne particle concentration.

Although it is possible to identify each plot from Fig. 2c and d, some experience is needed to interpret the RPs [53]. For this reason, recurrence quantification analysis (RQA) offers a window to characterise such RP structures.

The main idea of this project is to reconstruct the (unknown) system dynamics in the phase space by using time-delay embedding, and then computing the distances between all pairs of embedded vectors, generating a symmetric two-dimensional square matrix for each dataset as shown on Fig. 2c and d, applying RQA to each dataset.

3.1 Recurrence Quantification Analysis for RPs

Zbilut and Webber [53] have developed some of the methods used today for quantitative analysis of the recurrence plots. It has been shown that these measures are able to capture dynamical transitions in complex systems [54], defining measures of complexity using certain characteristics of the recurrence plots [25, 27].

In general, the characteristics measured in a RP are as follows: recurrence rate, determinism, ratio, entropy and trend. In this contribution, an extension of these characteristics was also considered such as laminarity and trapping time (TT).

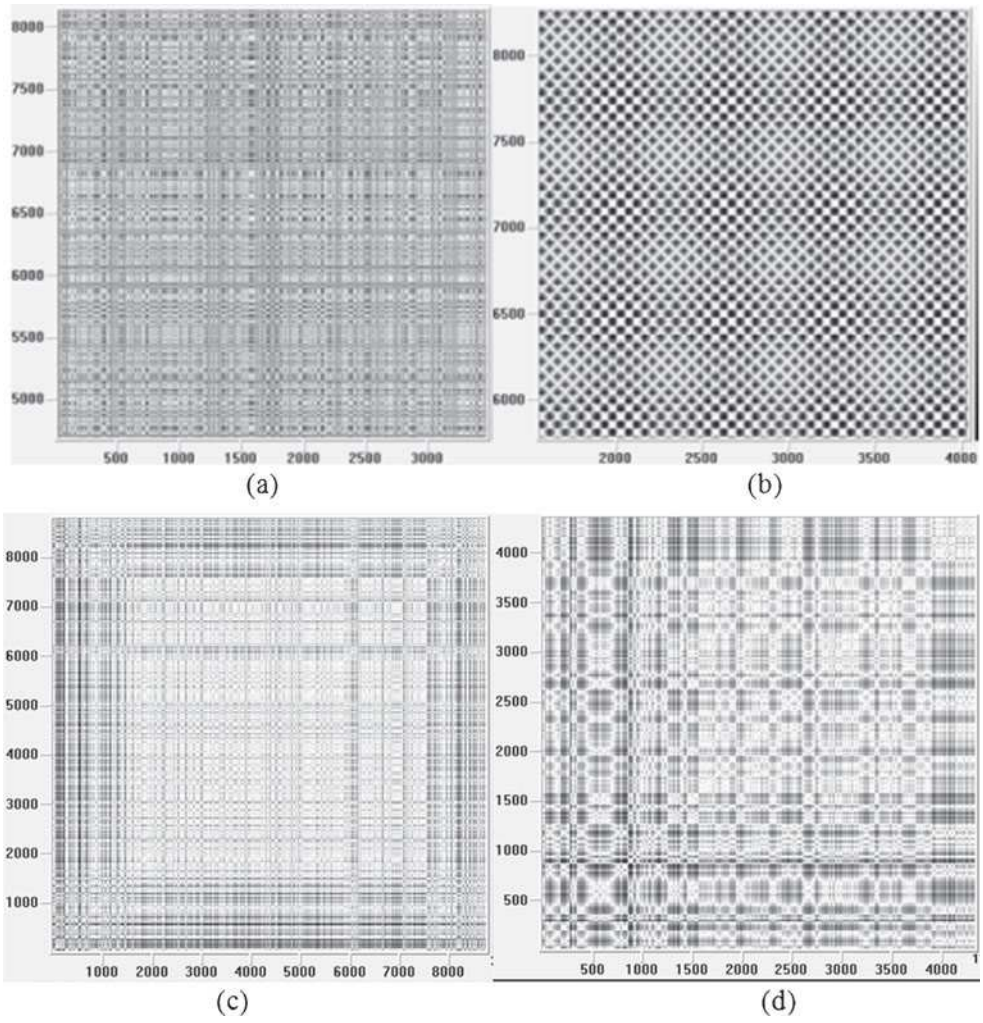

Fig. 2 Recurrence Plots using **a** random signal, **b** sine wave, **c** gas concentration of carbon monoxide at Mexico downtown for 2009, and **d** particle concentration of PM10 over 2010 at Mexico North East (daily mean) showing the Line of Identity (*diagonal line*). *X* and *Y* labels indicate hourly data points

3.2 Recurrence Rate

The recurrence rate is a measure of recurrences, or density of recurrence points in the RP. This rate gives the mean probability of recurrences in the system [27, 41]. The recurrence rate is given by:

$$RR(\varepsilon) = \frac{1}{N^2}\sum_{i,j=1}^{N} R_{i,j}(\varepsilon) \tag{2}$$

in the case of time series [28].

The recurrence rate represents the fraction of recurrent points with respect to the total number of possible recurrences. It is a density measure of the RP.

3.3 Determinism

Determinism is a measure for predictability of the system [5]. The determinism could also be explained as the percentage of recurrent points forming line segments which parallels the LOI. The determinism characteristic is given by [16]:

$$DET = \frac{\sum_{l=l_{\min}}^{N} lP^{\varepsilon}(l)}{\sum_{i,j}^{N} R_{i,j}^{m,e}} \tag{3}$$

Where $P(l)$ denotes the probability of finding a diagonal line of length l in the RP. This measure quantifies the predictability of a system [54]. The measure of determinism (DET) ranges from 0 to 1. Numbers near zero indicate randomness while those approaching 1 indicate the presence of a strong signal component [2, 14].

The average diagonal line length L_{mean} is defined as:

$$L_{mean} = \frac{\sum_{l=l_{min}}^{N} lP(l)}{\sum_{l=l_{min}}^{N} P(l)} \tag{4}$$

This characterises the average time that two segments of a trajectory stay in the vicinity of each other, and is related to the mean predictability time [54].

The choice of l_{min} can also be used in order to exclude short temporal scales that are not important [20].

3.4 Ratio

The ratio variable is defined as the quotient of DET divided by the recurrence (REC). It is useful to detect transitions between states: this ratio increases during transitions but settles down when a new quasi-steady state is achieved [31].

3.5 Entropy

The measured characteristic entropy refers to the Shannon entropy of the frequency distribution of the diagonal line lengths [50]. According to several authors, the basic idea is that information (Shannon) entropy of the random processes is abundantly supplied with the qualitative and quantitative data on the object under research [20, 26, 41, 50].

The entropy of a system is given by:

$$ENT = \sum_{l=l_{min}}^{N} p(l)\log p(l)\ with \quad p(l) = \frac{p^{\varepsilon}(l)}{\sum_{l=l_{min}}^{N} P^{\varepsilon}(l)} \tag{5}$$

3.6 Trend

The trend is a linear regression coefficient over the recurrence point density of the diagonals parallel to the LOI. The trend measurement is given by:

$$TREND = \frac{\sum_{i=1}^{N}\left(i - \frac{N}{2}\right)(RR_i = \{RR_i\})}{\sum_{i-1}^{N}\left(i = \frac{N}{2}\right)^2} \tag{6}$$

3.7 Laminarity

Laminarity may be defined as the amount of recurrence points which form vertical lines [31]. Thus, laminarity (LAM) can be quantified as expressed on Eq. 7

$$LAM = \frac{\sum_{v=v_{min}}^{N} v.P(v)}{\sum_{v=1}^{N} v.P(v)} \tag{7}$$

where $P(v)$ is the frequency distribution of the lengths v of the vertical lines, which have at least a length of $v_{\min}$. It is noteworthy that Laminarity is evidence of chaotic transitions and is related with the amount of laminar phases in the system (intermittency) [31].

3.8 Trapping Time

Trapping time shows the average length of the vertical lines and is given by Eq. 8:

$$TT = \frac{\sum_{v=v_{min}}^{N} vP(v)}{\sum_{v=v_{min}}^{N} P(v)} \tag{8}$$

Where v is the length of the vertical lines, v_{min} is the shortest length that is considered a line segment and $P(v)$ is

the distribution of the corresponding lengths. *TT* shows the time that the system has been trapped in the same state [20].

4 Experimental Results

Recurrence quantification analysis have been carried out for years 2005–2010 for all sites mentioned in section 2.2 for particles PM_{10}, CO, SO_2, NO_2, and O_3 using the raw data (hourly) obtained from the monitoring stations. The analysis has been carried out for REC, DET, ratio, TT, LAM and trend.

The results were analysed separately and presented in forms of boxplots according to two different approaches: by site and by type of particle. This analysis is complex due to the large quantity of the datasets. However, much useful information has been extracted from the recurrence plots using RQA.

4.1 Results by Monitoring Networks (Sites)

This approach explores the feasibility of using RQA to extract information from the recurrence plots by sites. As explained in Section 2.2, the monitoring networks were separated as: Northwest, Northeast, Downtown, Southwest, and Southeast. This approach does not take into account the type of particle, but rather the location of the monitoring network. Figure 3 shows the recurrence rate for all particles

Figure 3 shows the recurrence rate for all monitoring networks. In this figure, it is worth noticing that the median recurrence rate lies from 10 to 13, with the lowest recurrence rate being for Mexico Northwest. The other sites seem to have a fairly constant spread of the percentiles.

Figure 4 shows the determinism for years 2005–2010 by monitoring network shows a fairly constant mean for all sites. However, there are outliers for all sites showing an increase of over 80 in many cases. This exceptionally higher determinism may be explained in greater detail in the analysis by particle, which could give an insight of the reason this happened.

The ratio for particle concentration seems fairly stable for all sites ranging from 0 to 2 as a mean and the percentiles increasing up to 4 for some cases. The only exception for this drift is the monitoring station of the Northwest with ratios up to 10 and an outlier of about 38 (Fig. 5).

Furthermore, for entropy the frequency distribution of the data is also stable. Their median oscillates between 2 and 3 for all monitoring networks showing the percentiles reaching up to 5. This could also be due to the type of particle rather than the site. This is shown on Fig. 6

Figure 7 shows the trapping time for particle concentration separated by monitoring network. In this case, the average time that this non-linear system stays in the same state seems fairly constant with a low median between 10 and 13. It is also worth noting that for most sites, there are outliers which cannot be explained in detail using this approach.

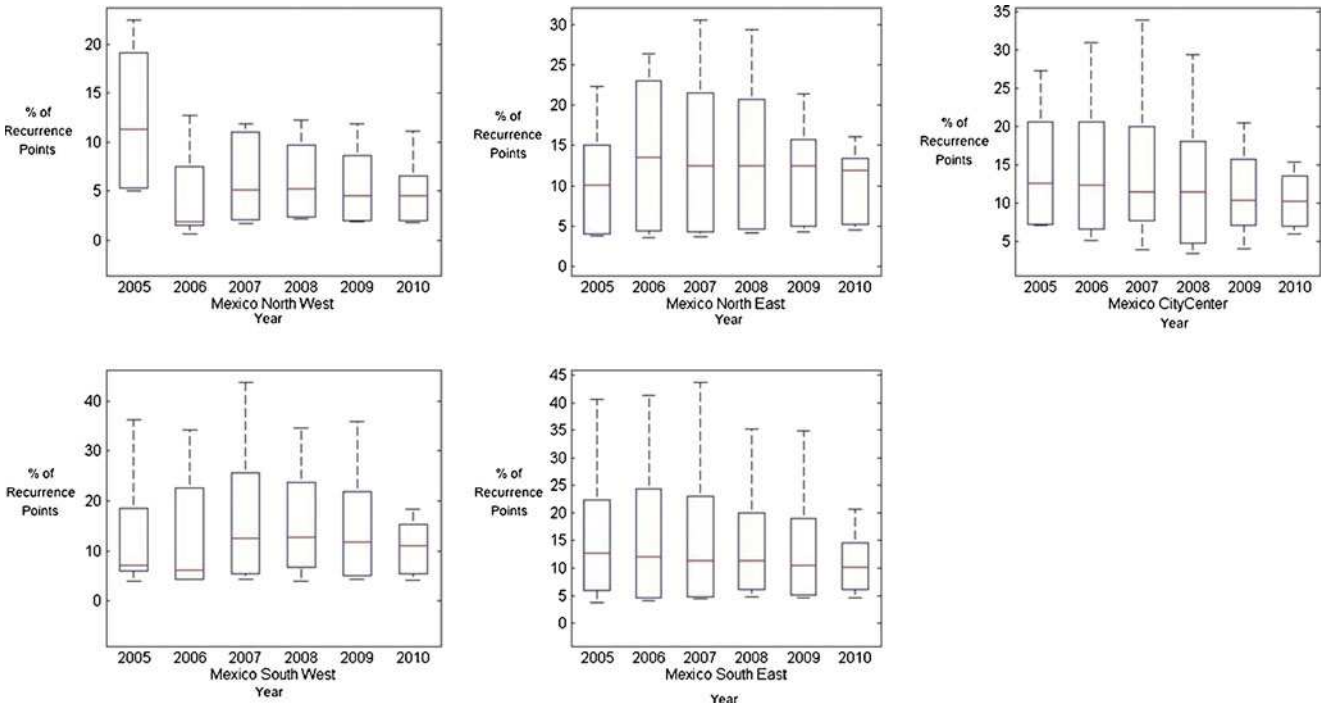

Fig. 3 Recurrence rate, years 2005–2010 by monitoring site. All five sites are shown (years vs. percentage of recurrence points). There is one *box* for each site and the boxes have *lines* at the *lower quartile*, *median*, and *upper quartile values*. The *whiskers* are lines extending from each end of the boxes to show the extent of the rest of the data. *Outliers* are data with values beyond the ends of the *whiskers*

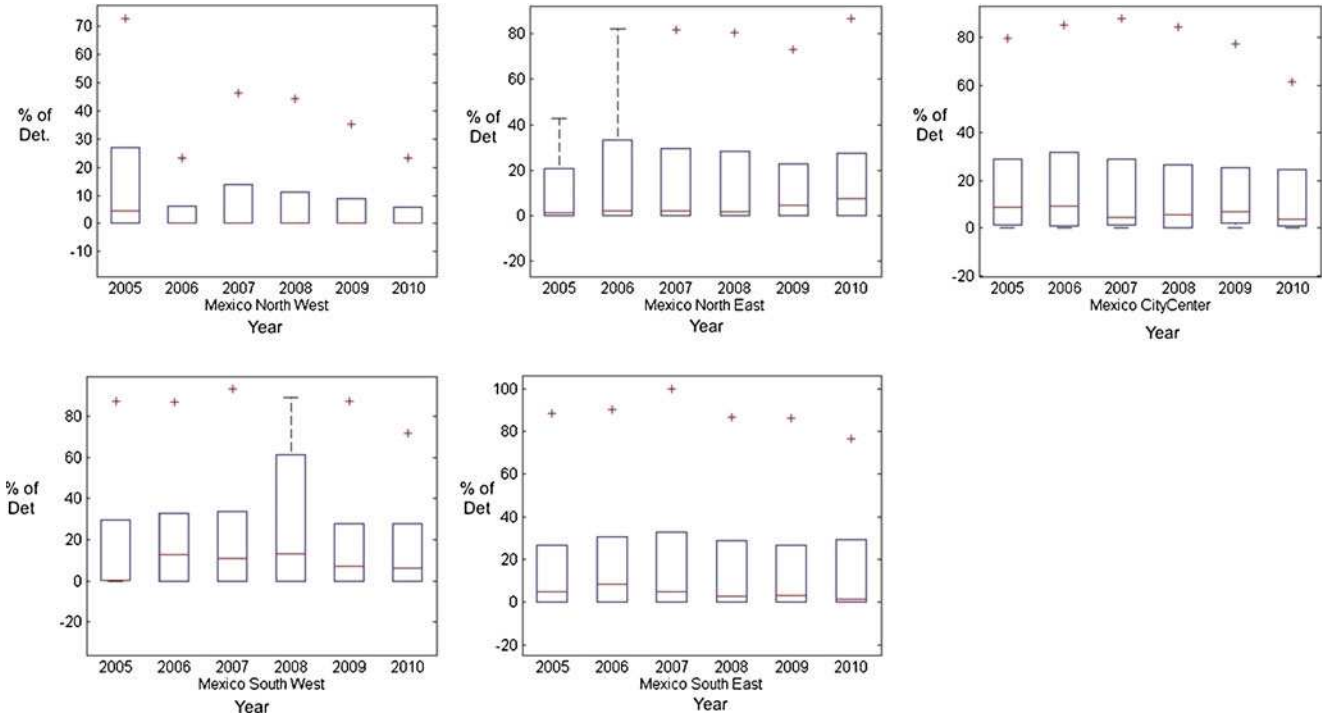

Fig. 4 Determinism, years 2005–2010 by monitoring site. All five sites are shown (years vs. percentage of determinism). There is one *box* for each site and the boxes have *lines* at the *lower quartile*, *median*, and *upper quartile values*. The *whiskers* are lines extending from each end of the boxes to show the extent of the rest of the data. *Outliers* are data with values beyond the ends of the *whiskers*

Figure 8 shows the laminarity for particle concentration by monitoring network. Since the laminarity is the measurement of chaotic transitions, it can be inferred that regardless of the site, the changes in laminar phases in the system seem high.

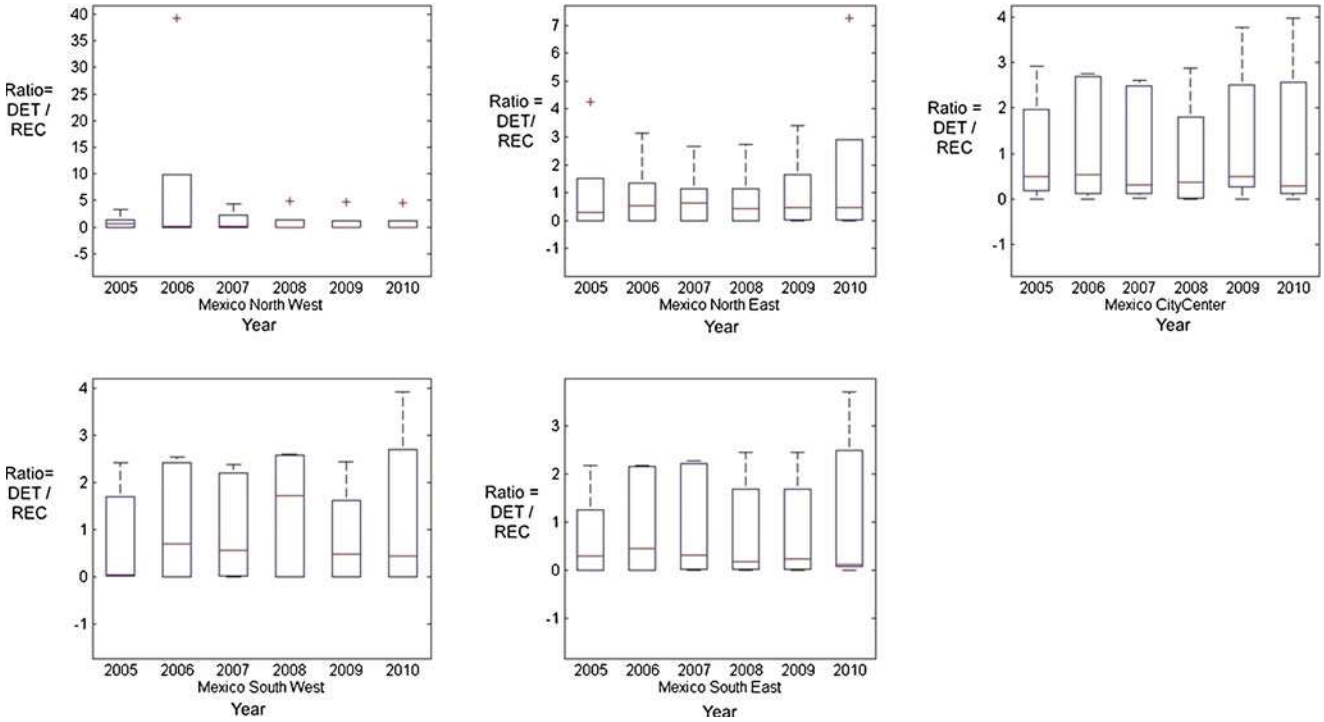

Fig. 5 Ratio for particle concentration, years 2005–2010 by monitoring site. All five sites are shown (years vs. ratio). There is one *box* for each site and the boxes have *lines* at the *lower quartile*, *median*, and *upper quartile values*. The *whiskers* are lines extending from each end of the boxes to show the extent of the rest of the data. *Outliers* are data with values beyond the ends of the *whiskers*

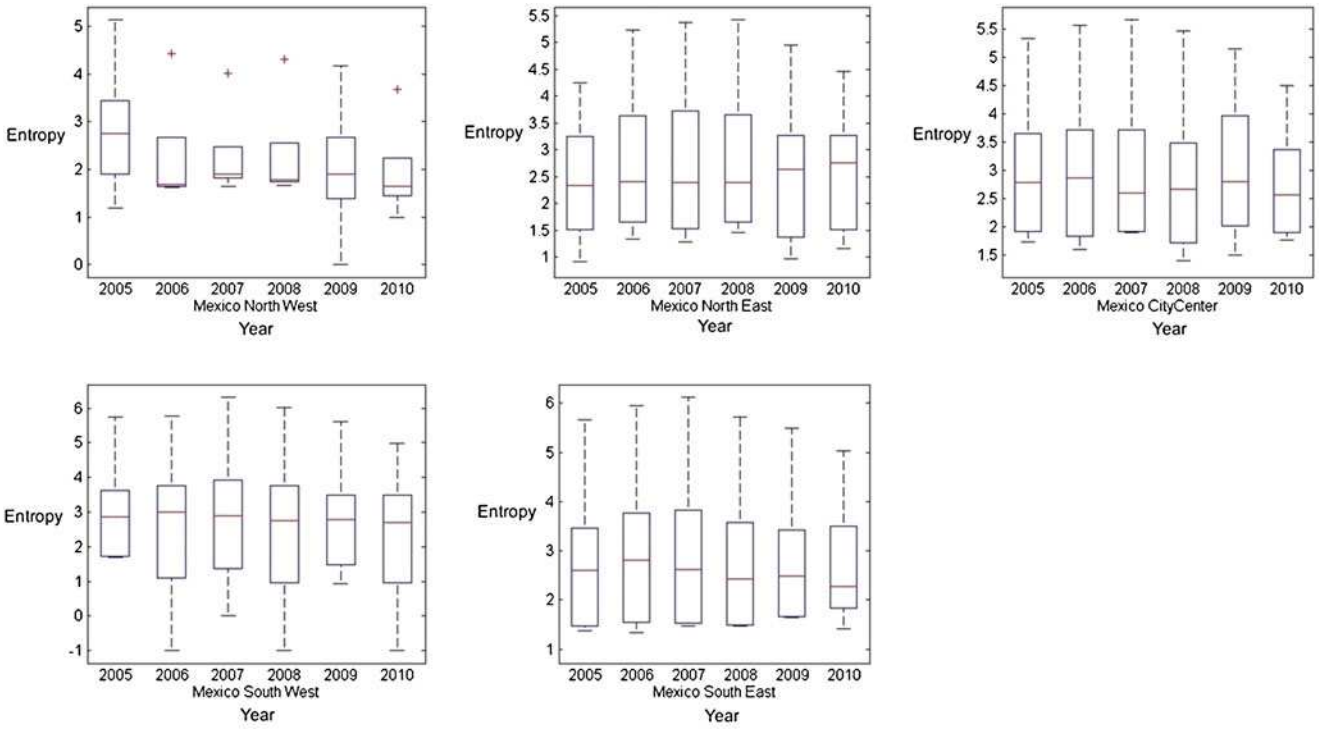

Fig. 6 Entropy for particle concentration, years 2005–2010 by monitoring site. All five sites are shown (years vs. entropy). There is one *box* for each site and the boxes have *lines* at the *lower quartile*, *median*, and *upper quartile values*. The *whiskers* are lines extending from each end of the boxes to show the extent of the rest of the data. *Outliers* are data with values beyond the ends of the *whiskers*

The last measure for this approach was the trend. Since the trend represents the measure of the positioning of recurrent points away from the central diagonal, that is the paling of the RP towards its edges [31]. A "flat" diagram indicates stationarity,

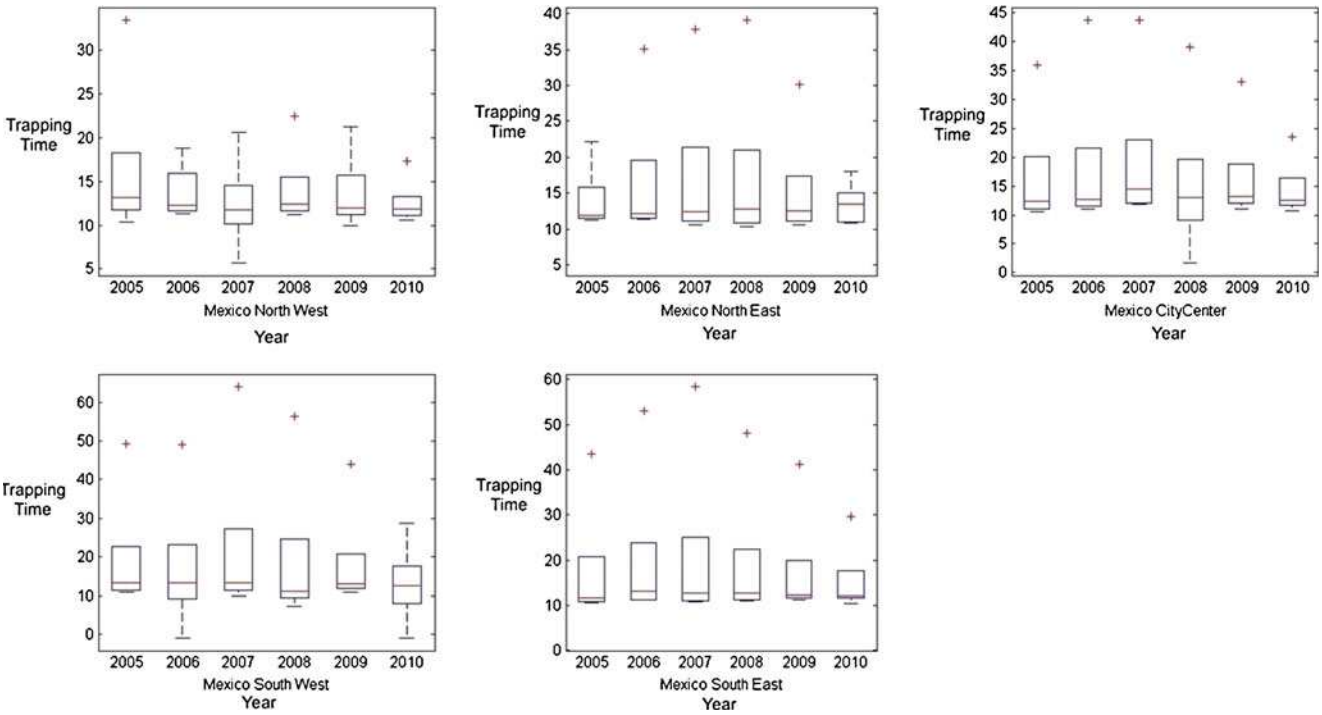

Fig. 7 Trapping time for particle concentration, years 2005–2010 by monitoring site. All five sites are shown (years vs. trapping time). There is one *box* for each site and the boxes have *lines* at the *lower quartile*, *median*, and *upper quartile values*. The *whiskers* are lines extending from each end of the boxes to show the extent of the rest of the data. *Outliers* are data with values beyond the ends of the *whiskers*

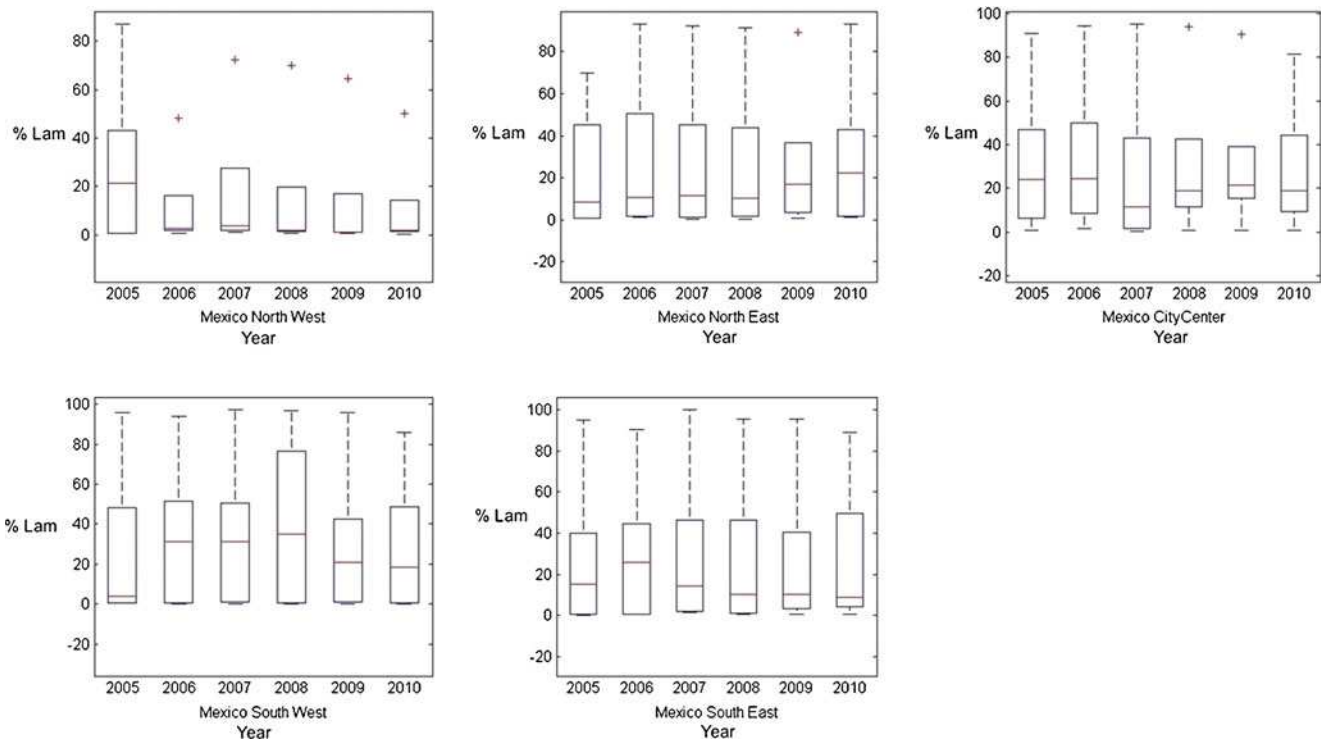

Fig. 8 Laminarity for particle concentration, years 2005–2010 by monitoring site. All five sites are shown (years vs. laminarity). There is one *box* for each site and the boxes have *lines* at the *lower quartile*, *median*, and *upper quartile values*. The *whiskers* are lines extending from each end of the boxes to show the extent of the rest of the data. *Outliers* are data with values beyond the ends of the *whiskers*

whereas a drift in the signal will result in the overall increase or reduction of distances as the signal is moved away from the main diagonal. In this respect, it could be noticed that most of the sites have a median between 11 and 14. This is shown on Fig. 9.

4.2 Results by Particle Types

For this approach, the recurrence quantification analysis is carried out by particle type. In Fig. 10, the recurrence rate by particle type is shown. This figure shows the recurrence rate for all five particles (CO, O_3, NO_2, SO_2 and PM_{10}.) It is worth noticing that the median recurrence rate for all particles varies. For CO, the median lies between 13 and 18, with a slight increase in recurrence over the years. This is consistent with the findings of other authors [24, 40] where CO levels decreased overall on a long-term average. Both ozone and PM_{10} shows a low recurrence rate below 6 for all years, regardless of the monitoring sites. Nitrogen dioxide shows a slightly higher recurrence with a median between 10 and 12. The behaviour of nitrogen dioxide seems to concur with the slight decrease of this gas over the years found by other authors [40].

However, sulphur dioxide shows a median above 30 for some years. This explains Fig. 3, where the whiskers of the boxplots show a much higher recurrence in some cases, these cases being for sulphur dioxide. This higher recurrence rate may be due to the low variances in values of the datasets for all years, making it easier for RQA to determine recurrence. These results for recurrence seem to indicate that the overall increase on the long-term behaviour of the particular gas relates to the decrease of the gas level.

Furthermore, the determinism for SO_2 is also much higher than for other particles, having a median between 70 and 90 as shown on Fig. 11. Although it seems lower due to the scaling of the boxplots, the median shows otherwise, the spread in the 25th to 75th percentiles and the length of the whiskers may be due to high variances in the datasets for that type of particle. This could also indicate that SO_2 may be more predictable than the other particles.

Furthermore, it is worth noticing for entropy (Fig. 12) that the frequency distribution of the data is slightly higher for sulphur dioxide as well. The other particles seem to have steady entropy whose median oscillates between 1 and 3.

Figure 13 shows the trapping time separated by particle type. For this figure, it can be seen that sulphur dioxide shows also a much higher trapping time showing a median of 40 for some years (e.g., 2008 and 2009) in comparison with the other particles between 10 and 13. This explains the outliers seen on Fig. 7, which could not be explained using the monitoring networks' approach.

Figure 14 shows the laminarity for particle concentration by particle type. In this figure, it is shown that for carbon monoxide and PM_{10} the chaotic transitions are high, especially for

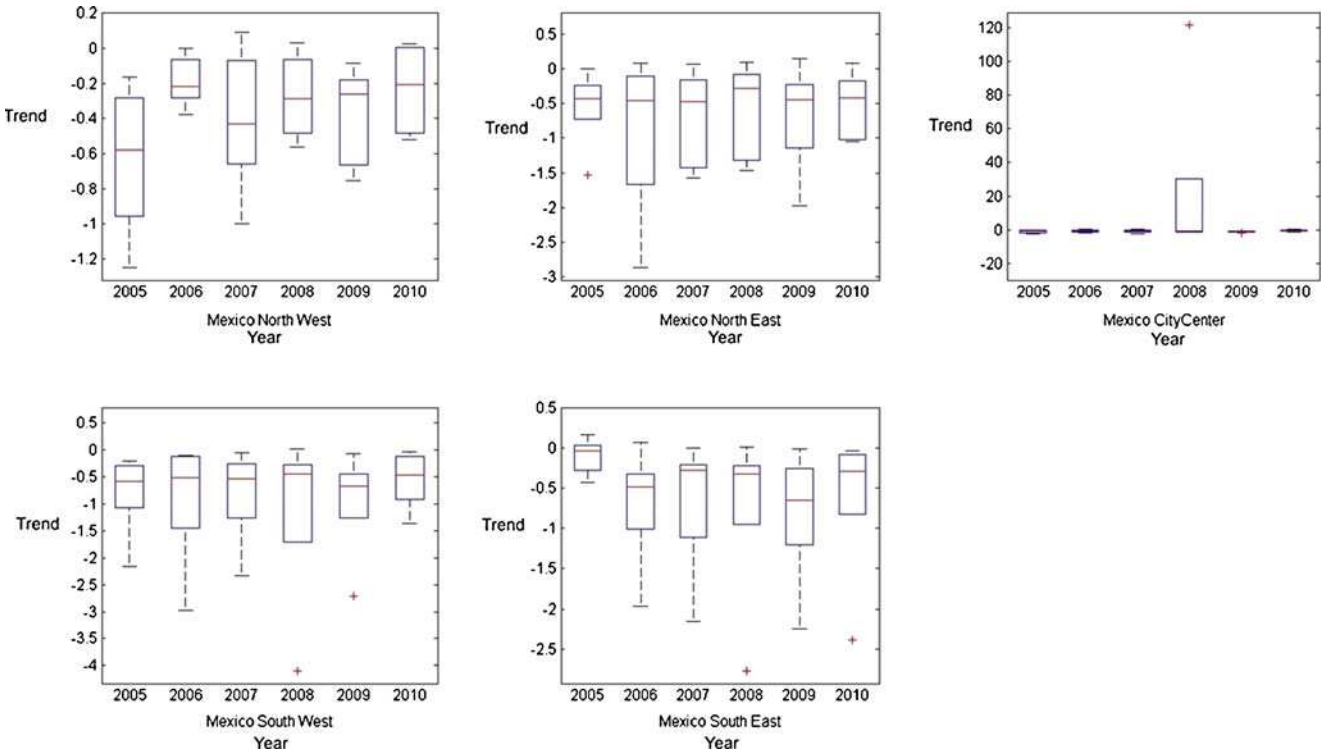

Fig. 9 Trend for particle concentration, years 2005–2010 by monitoring site. All five sites are shown (years vs. trend). There is one *box* for each site and the boxes have *lines* at the *lower quartile*, *median*, and *upper quartile values*. The *whiskers* are lines extending from each end of the boxes to show the extent of the rest of the data. *Outliers* are data with values beyond the ends of the *whiskers*

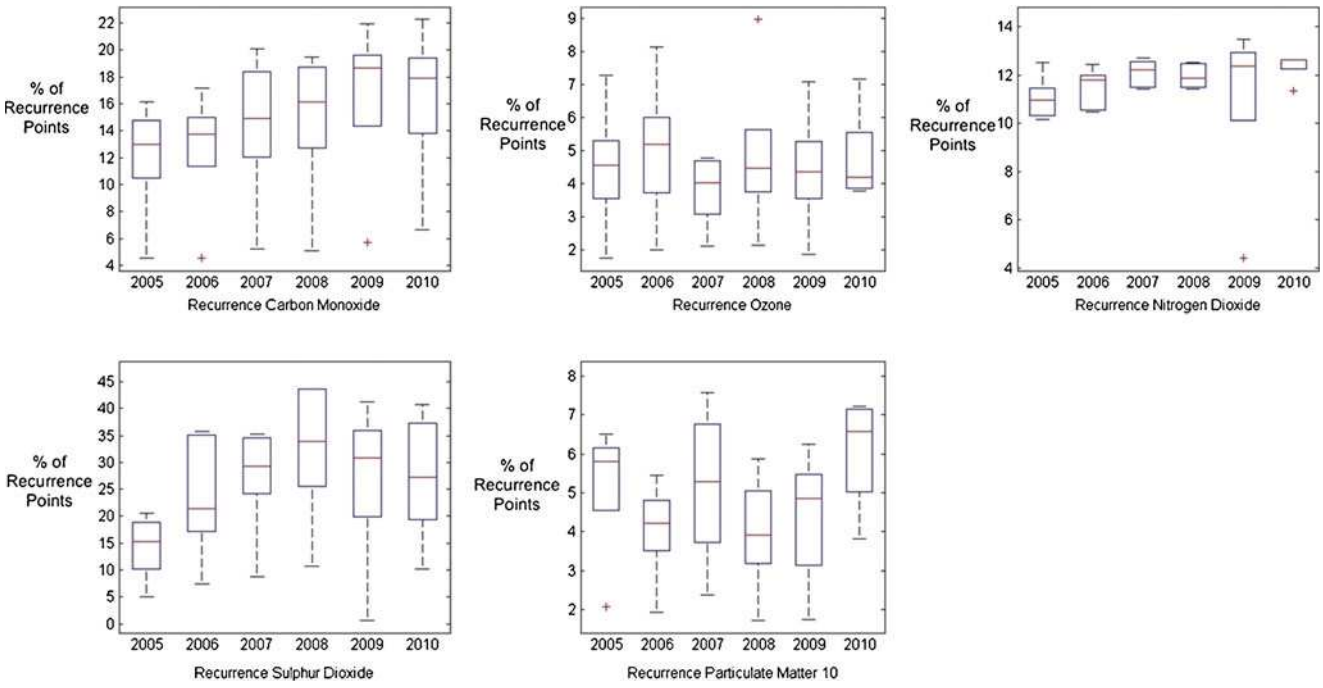

Fig. 10 Recurrence rate for particle concentration, years 2005–2010 by particle type. All five gases are shown (years vs. percentage of recurrence points). There is one *box* for each site and the boxes have *lines* at the *lower quartile*, *median*, and *upper quartile values*. The *whiskers* are lines extending from each end of the boxes to show the extent of the rest of the data. *Outliers* are data with values beyond the ends of the *whiskers*

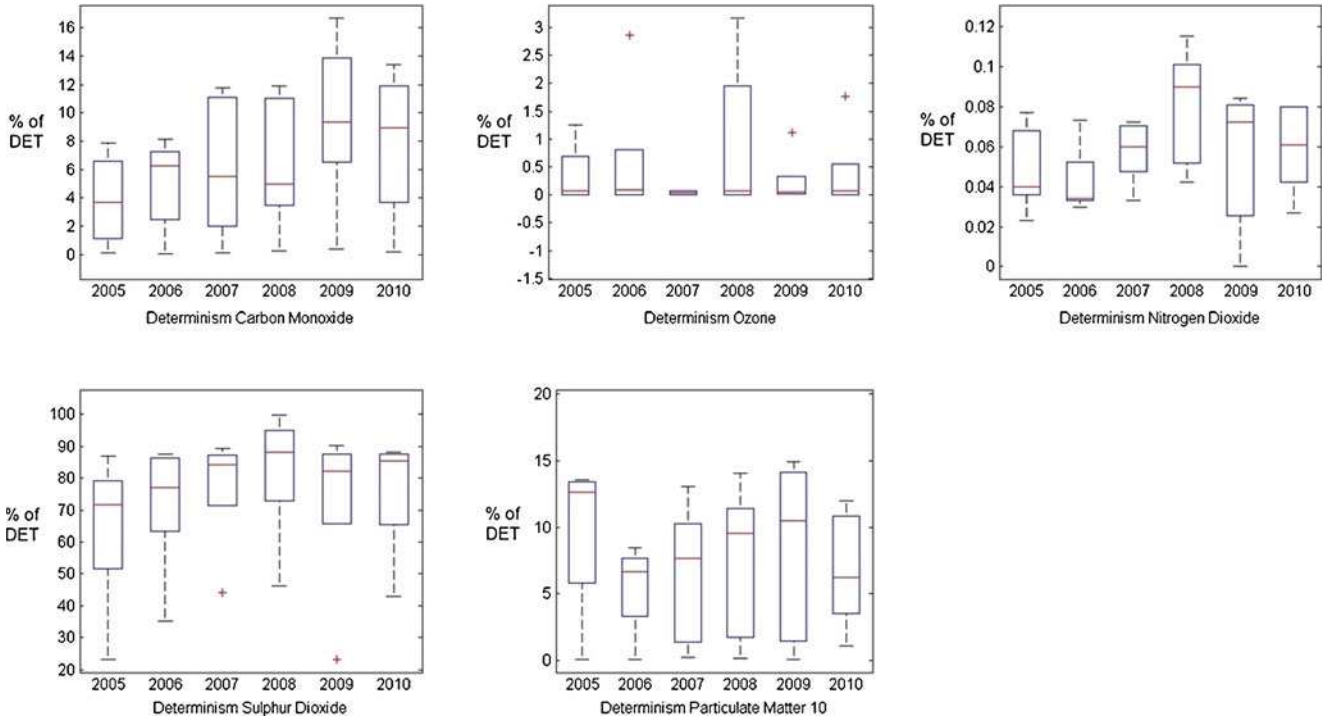

Fig. 11 Determinism for particle concentration, years 2005–2010 by particle type. All five gases are shown (years vs. percentage of recurrence points). There is one *box* for each site and the boxes have *lines* at the *lower quartile*, *median*, and *upper quartile values*. The *whiskers* are lines extending from each end of the boxes to show the extent of the rest of the data. *Outliers* are data with values beyond the ends of the *whiskers*

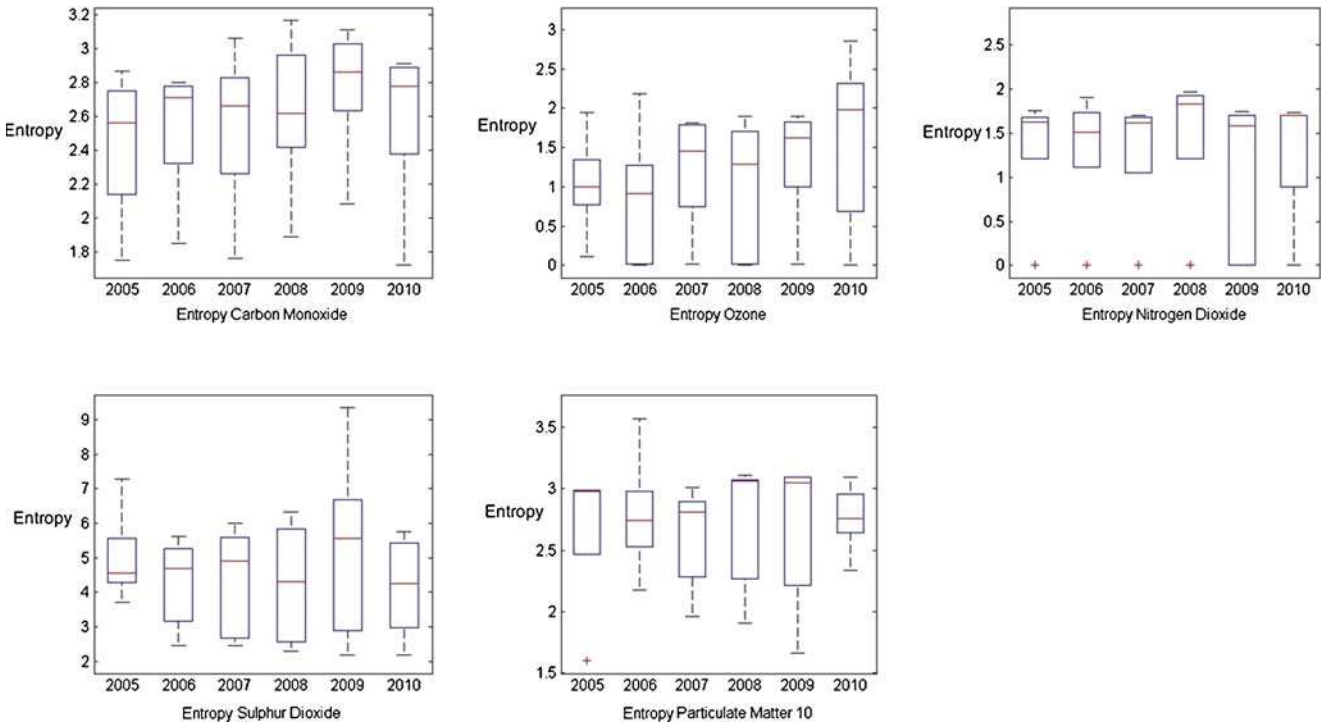

Fig. 12 Entropy for particle concentration, years 2005–2010 by particle type. All five gases are shown (years vs. percentage of entropy). There is one *box* for each site and the boxes have *lines* at the *lower quartile*, *median*, and *upper quartile values*. The *whiskers* are lines extending from each end of the boxes to show the extent of the rest of the data. *Outliers* are data with values beyond the ends of the *whiskers*

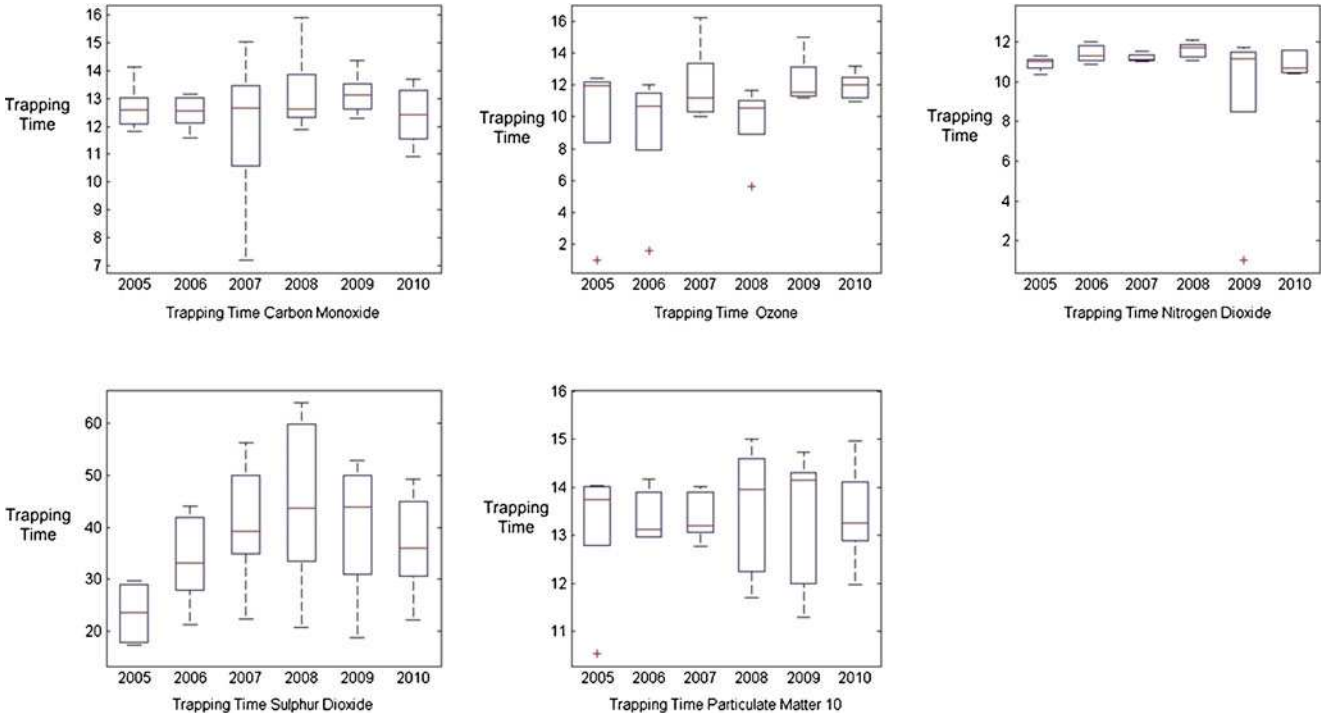

Fig. 13 Trapping time for particle concentration, years 2005–2010 by particle type. All five gases are shown (years vs. percentage of trapping time). There is one *box* for each site and the boxes have *lines* at the *lower quartile*, *median*, and *upper quartile values*. The *whiskers* are lines extending from each end of the boxes to show the extent of the rest of the data. *Outliers* are data with values beyond the ends of the *whiskers*

sulphur dioxide. This gives another insight of the chaotic transitions, since Fig. 8 shows that the laminarity is high for all sites, in Fig. 14, it can be explained that only some particles gives this high changes in laminar phases.

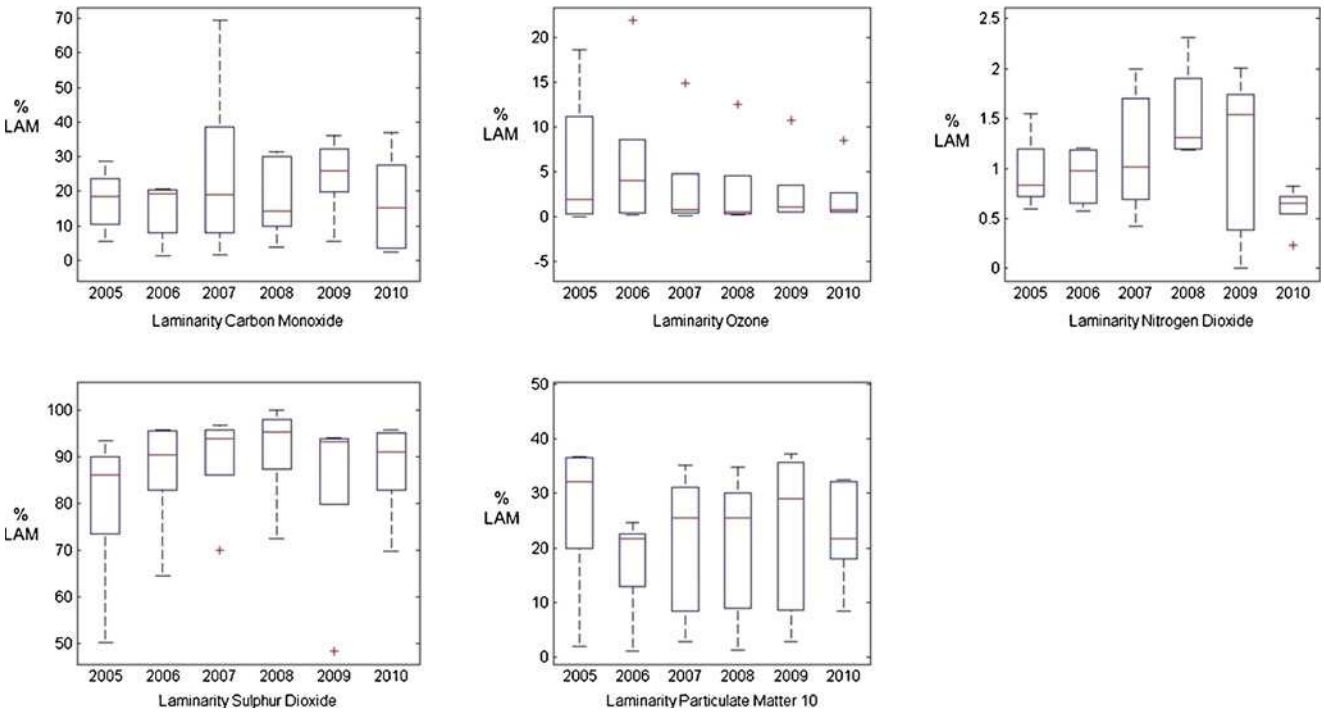

Fig. 14 Laminarity for particle concentration, years 2005–2010 by particle type. All five gases are shown (years vs. percentage of laminarity). There is one *box* for each site and the boxes have *lines* at the *lower quartile*, *median*, and *upper quartile values*. The *whiskers* are lines extending from each end of the boxes to show the extent of the rest of the data. *Outliers* are data with values beyond the ends of the *whiskers*

5 Conclusions and Future Work

Numerous experiments have been carried out with different gases and through different years. Using recurrence quantification analysis, it could be shown that information could be extracted from large datasets of dissimilar airborne particles during a considerable time lap (6 years, in this case) for five monitoring sites. Trends could be identified using these tools and preliminary conclusions suggest that important information such as density distribution and drifts, among others, could be drawn. Also, using more than one approach, some hidden features could be identified showing the feasibility of this approach.

A much higher determinism for SO_2 indicates a greater measure of predictability of the gas. This means that the ability of RQA to extract density distributions, decrease in the amount of gas, etc. could be deterministic-dependent. This could be the reason recurrence tools analyses of other gases were not clear.

Approach by monitoring site does not always give much useful information unless it is co-reviewed with the type of particle approach.

Preliminary results shown for recurrence seem to indicate that the overall increase on the long-term behaviour of the particular gas relates to the decrease of the gas level. This long-term behaviour needs further investigation, but it was clear that a relationship exists between the increase of the recurrence percentage and the decrease in the gas level.

For future work, it could be useful to use a combination of RQA with prediction algorithms such as support vector machines to carry out prognosis of the airborne particle data. Another useful approach that could be carried out is the use of cross recurrence plot, making a comparison between two recurrence plots to determine trends and further investigate the findings in this paper.

Acknowledgments The authors would like to acknowledge the financial support of the Mexican government via PROMEP funding.

References

1. Aboofazeli, M., & Moussavi, Z. K. (2008). Comparison of recurrence plot features of swallowing and breath sounds. *Chaos, Solitons and Fractals, 37*, 454–464.
2. Ahlstrom, C., Höglund, K., Hult, P., Häggström, J., Kvart, C., & Ask, P. (2006). Distinguishing innocent murmurs from murmurs caused by aortic stenosis by recurrence quantification analysis. *World Academy of Science, Engineering and Technology, 18*, 40–45.
3. Ahmad, S. S., Biiker, P., Emberson, L., & Rabia, S. (2011). Monitoring nitrogen dioxide levels in urban areas in Rawalpindi, Pakistan. *Water, Air, and Soil Pollution, 220*, 141–150.
4. Achcar, J. A., Sousa, D. E. F., Rodrigues, E. R., & Tzintzun, G. (2011). Comparing the number of ozone exceedances in different seasons of the year in Mexico City. *Environmental Modeling and Assessment, 16*, 251–264.
5. Aparicio, T., Pozo, E. F., & Saura, D. (2008). Detecting determinism using recurrence quantification analysis: three test procedures. *Journal of Economic Behavior & Organization, 65*, 768–787.
6. Arbex, M. A., Nascimento Saldiva, P. H., Amador Pereira, L. A., & Ferreira Braga, A. L. (2010). Impact of outdoor biomass air pollution on hypertension hospital admissions. *Journal of Epidemiology and Community Health, 64*, 573–579.
7. Bell, M. L., Goldberg, R., Rogrefe, C., Kinney, P. L., Knowlton, K., Lynn, B., et al. (2007). Climate change, ambient ozone, and health in 50 US cities. *Climate Change, 82*, 61–76.
8. Bell, M. L., Peng, R. D., Dominici, F., & Samet, J. M. (2009). Emergency hospital admissions for cardiovascular diseases and ambient levels of carbon monoxide : results for 126 United States Urban Counties, 1999–2005. *Circulation, 120*, 949–955.
9. Boubel, R. W., Fox, D. L., Turner, D. B., & Stern, A. C. (1994). *Fundamentals of air pollution* (3rd ed.). New York: Academic Press, Waltham.
10. Bradley, E., & Mantilla, R. (2002). Recurrence plots and unstable periodic orbits. *Chaos, 12–3*, 596–600.
11. Chambers, C. A., Hopkins, R. O., Weaver, L. K., & Key, C. (2008). Cognitive and affective outcomes of more severe compared to less severe carbon monoxide poisoning. *Brain Injury, 22*, 387–395.
12. Chiusolo, M., Cadum, E., Stafoggia, M., Galassi, C., Berti, G., Faustini, A., Bisanti, L., Vigotti, M. A., Dessì, M. P., Cernigliaro, A., Mallone, S., Pacelli, B., Minerba, S., Simonato, L., & Forastiere, F. (2011). Short-term effects of nitrogen dioxide on mortality and susceptibility factors in 10 Italian cities: the EpiAir study. *Environ Health Perspect, 119*(19), 1233–1238.
13. Eckmann, J. P., Kamphorst, S. O., & Ruelle, D. (1987). Recurrence plots of dynamical systems. *Europhysics Letters, 4*, 324–327.
14. Furman, M. D., Simonotto, J. D., Beaver, T. M., Spano, M. L., & Ditto, W. L. (2006). Using recurrence quantification analysis determinism for noise removal in cardiac optical mapping. *IEEE Trans Biomed Eng, 53*(4), 767–770.
15. Emberson, L., Ashmore, M., & Murray, F. (Eds.). (2003). *Air pollution impacts on crops and forests: a global assessment* (Air pollution reviews, Vol. 4). London: Imperial College Press.
16. Gao, J., & Cai, H. (2000). On the structures and quantification of recurrence plots. *Physics Letters A, 270*, 75–87.
17. Gold, D. R., Damokosh, A. I., Pope, C. A., Dockery, D. W., McDonnell, W. F., Serrano, P., Retama, A., & Castillejos, M. (1999). Particulate and ozone pollutant effects on the respiratory function of children in Southwest Mexico City. *Epidemiology, 10*(8), 8–16.
18. Guo, Y., Barnett, A. G., Zhang, Y., Tong, S., Yu, W., & Pan, X. (2010). The short-term effect of air pollution on cardiovascular mortality in Tianjin, China: comparison of time series and case–crossover analyses. *Science of the Total Environment, 409*, 300–306.
19. Jones, A. M., & Harrison, R. M. (2011). Temporal trends in sulphate concentrations at European sites and relationships to sulphur dioxide. *Atmospheric Environment, 45*, 873–882.
20. Karakasidis, T. E., Liakopoulos, A., Fragkou, A., & Papanicolaou, P. (2009). Recurrence quantification analysis of temperature fluctuations in a horizontal round heated turbulent jet. *International Journal of Bifurcation and Chaos, 19–8*, 2487–2498.
21. Kilabuko, J. H., Matsuki, H., & Nakai, S. (2007). Air quality and acute respiratory illness in biomass fuel using homes in Bagamoyo, Tanzania. *International Journal of Environmenal Research Public Health, 4*(1), 39–44.
22. Lee, Y. L., Wanga, W.-H., Luc, C.-W., Lina, Y.-H., & Hwang, B.-F. (2011). Effects of ambient air pollution on pulmonary function among schoolchildren. *International Journal of Hygiene and Environmental Health, 214*, 369–375.
23. Liu, Y.-J., & Harrison, R. M. (2011). Properties of coarse particles in the atmosphere of the United Kingdom. *Atmospheric Environment, 45*, 3267–3276.

24. Madronich, S. (2006). Chemical evolution of gaseous air pollutants down-wind of tropical megacities: Mexico City case study. *Atmospheric Environment, 40*, 6012–6018.
25. March, T. K., Chapman, S. C., & Dendy, R. O. (2005). Recurrence plot statistics and the effect of embedding. *Physica D, 200*, 171–184.
26. Marwan, N., Thiel, M., & Nowaczyk, N. R. (2002). Cross recurrence plot based synchronization of time series. *Nonlinear Processes in Geophysics, 9*, 325–331.
27. Marwan, N., Romano, M. C., Thiel, M., & Kurths, J. (2007). Recurrence plots for the analysis of complex systems. *Physics Reports, 438*, 237–329.
28. Mocenni, C., Facchini, A., & Vicino, A. (2011). Comparison of recurrence quantification methods for the analysis of temporal and spatial chaos. *Mathematical and Computer Modelling, 53*, 1535–1545.
29. NOM (2002). Modificación a la Norma Oficial Mexicana NOM-020-SSA1-1993. Diario Oficial de la Federación. 30 de Octubre de 2002.
30. O'Neill, M. R., Loomis, D., & Borja-Aburto, V. H. (2004). Ozone, area social conditions and mortality in Mexico City. *Environmental Research, 94*, 234–242.
31. Palmieri, F., & Fiore, U. (2009). A nonlinear, recurrence-based approach to traffic classification. *Computer Networks, 53*, 761–773.
32. Peng, G., Wang, X., Wu, Z., Wang, Z., Yang, L., Zhong, L., & Chen, D. (2011). Characteristics of particulate matter pollution in the Pearl River Delta region, China: an observational-based analysis of two monitoring sites. *Journal of Environmental Monitoring, 13*, 1927.
33. Pey, J., Alastuey, A., Querol, X., & Rodríguez, S. (2010). Monitoring of sources and atmospheric processes controlling air quality in an urban Mediterranean environment. *Atmospheric Environment, 44*, 4879–4890.
34. Rao, D., & Phipatanakul, W. (2011). Impact of environmental controls on childhood asthma. *Current Allergy and Asthma Reports, 11*, 414–420.
35. Rao, P. S., Ansari, M. F., Gajrani, C. P., Kumar, A., Nema, P., & Devotta, S. (2006). Atmospheric concentrations of sulphur dioxide in and around a typical Indian petroleum refinery. *Bulletin of Environmental Contamination and Toxicology, 77*, 274–281.
36. Romieu, I., Meneses, F., Ruiz-Velazco, S., Sierra-Monge, J. J., Huerta, J., White, M. C., & Etzel, R. (1996). Effects of air pollution on the respiratory health of asthmatic children living in Mexico City. *American Journal of Respiratory and Critical Care Medicine, 154*, 300–307.
37. Samoli, E., Touloumi, G., Schwartz, J., Anderson, H. R., Schindler, C., Forsberg, B., Vigotti, M. A., Vonk, J., Kosnik, M., Skorkovsky, J., & Katsouyanni, K. (2007). Short-term effects of carbon monoxide on mortality: an analysis within the APHEA project. *Environmental Health Perspectives, 115*, 1578–1583.
38. SIMAT (2010). Sistema de Monitoreo Atmosférico (Atmospheric Monitoring System), Annual technical report, Mexico City, Mexico, pp. 1–166.
39. Smith, S. J., Conception, E., Andres, R., Lurz, J. (2004). Historical sulfur dioxide emissions 1850–2000: Methods and results PNNL research report, Pacific Northwest National Laboratoy.
40. Stephens, S., Madronich, S., Wu, F., Olson, J., Ramos, R., Retama, A., & Munoz, R. (2008). Weekly patterns of Mexico City's surface concentrations of CO, NOx, PM10 and O3 during 1986–2007. *Atmospheric Chemistry and Physics Discussion, 8*, 8357–8384.
41. Strozzi, F., Zaldıvar, J. M., & Zbilut, J. P. (2007). Recurrence quantification analysis and state space divergence reconstruction for financial time series analysis. *Physica A, 376*, 487–499.
42. Suh, H. H., Zanobetti, A., Schwartz, J., & Coull, B. A. (2011). Chemical properties of air pollutants and cause-specific hospital admissions among the elderly in Atlanta, Georgia. *Environ Health Perspect, 119*(10), 1421–1428.
43. Takizawa, H. (2011). Impact of air pollution on allergic diseases. *Korean Journal of Internal Medicine, 26*, 262–273.
44. Tanio, M., Hirata, Y., & Hideyuki, S. (2009). Recurrence plot statistics and the effect of embedding. *Physics Letters A, 373*, 2031–2040.
45. United States Environmental Protection Agency (USEPA) (2000). Air quality criteria for carbon monoxide. National Center for Environmental Assessment, Office of Research and Development. Research Triangle Park, NC, USA, June. Report No. EPA 600/P-99/001F.
46. United States Environmental Protection Agency (USEPA) (2006) Air quality criteria for ozone and related photochemical oxidants. Volume I. National Center for Environmental Assessment-RTP Office of Research and Development. Research Triangle Park, NC, USA, February.
47. Varon, J., Marik, P. E., Fromm, R. E., & Gueler, A. (1999). Carbon monoxide poisoning: a review for clinicians. *The Journal of Emergency Medicine, 17*, 87–93.
48. Vestreng, V., Myhre, G., Fagerli, H., Reis, S., & Tarrason, L. (2007). Twenty-five years of continuous sulphur dioxide emission reduction in Europe. *Atmospheric Chemistry and Physics, 7*, 3663–3681.
49. Weinmayr, G., Romeo, E., De Sario, M., Weiland, S. K., & Forastiere, F. (2010). Short-term effects of PM10 and NO2 on respiratory health among children with asthma or asthma-like symptoms: a systematic review and meta-analysis. *Circulation, 121*, 2331–2378.
50. Yulmetyev, R. M., & Gafarov, F. M. (1999). Dynamics of the information entropy in random processes. *Physica A, 273*, 416–438.
51. Zbilut, J. P., Thomasson, N., & Webber, C. L. (2002). Recurrence quantification analysis as a tool for nonlinear exploration of nonstationary cardiac signals. *Medical Engineering & Physics, 24*, 53–60.
52. Zbilut, P., Zaldivar-Comenges, J.-M., & Strozzi, F. (2007). Recurrence quantification based Liapunov exponents for monitoring divergence in experimental data. *Physics Letters A, 297*, 173–181.
53. Zbilut, J. P., & Webber, C. L., Jr. (2007). Recurrence quantification analysis: introduction and historical context. *International Journal of Bifurcation and Chaos, 17*(10), 3477–3481.
54. Zou, Y., Donner, R. V., Donges, J. F., Marwan, N., & Kurths, J. (2010). Identifying complex periodic windows in continuous-time dynamical systems using recurrence-based methods. *Chaos, 20*, 043130.